

# A CP-violating phase in a two Higgs triplet scenario : some phenomenological implications

Avinanda Chaudhuri <sup>1</sup> and Biswarup Mukhopadhyaya <sup>2</sup>

*Regional Centre for Accelerator-based Particle Physics  
Harish-Chandra Research Institute  
Chhatnag Road, Jhusi, Allahabad - 211 019, India*

## Abstract

We consider a scenario where, along with the usual Higgs doublet, two scalar triplets are present. The extension of the triplet sector is required for the Type II mechanism for the generation of neutrino masses, if this mechanism has to generate a neutrino mass matrix with two-zero texture. One CP-violating phase has been retained in the scalar potential of the model, and all parameters have been chosen consistently with the observed neutrino mass and mixing patterns. We find that a large phase ( $\gtrsim 60^\circ$ ) splits the two doubly-charged scalar mass eigenstates wider apart, so that the decay  $H_1^{++} \rightarrow H_2^{++}h$  is dominant (with  $h$  being the 125 GeV scalar). We identify a set of benchmark points where this decay dominates. This is complementary to the situation, reported in our earlier work, where the heavier doubly-charged scalar decays as  $H_1^{++} \rightarrow H_2^+W^+$ . We point out the rather spectacular signal, ensuing from  $H_1^{++} \rightarrow H_2^{++}h$ , in the form of Higgs plus same-sign dilepton peak, which can be observed at the Large Hadron Collider.

---

<sup>1</sup>E-mail: avinanda@hri.res.in

<sup>2</sup>E-mail: biswarup@hri.res.in

# 1 Introduction

The observation of a rather distinctive pattern of neutrino mixing, together with the available information on neutrino mass splitting, has triggered numerous theoretical proposals going beyond the standard electroweak model (SM). Seesaw models enjoy a fair share of these, along with additional assumptions to suit particular textures of the neutrino mass matrix.

Type-II seesaw models can generate Majorana neutrino masses without any right-handed neutrino(s), with the help of one or more  $Y=2$  scalar triplets. The restriction of the vacuum expectation value (vev) of such a triplet, arising from the limits on the  $\rho$ -parameter (with  $\rho = m_W^2/m_Z^2 \cos^2 \theta$ ), is obeyed in a not so unnatural manner, where the constitution of the scalar potential can accommodate large triplet scalar masses vis-a-vis a small vev. In fact, this very feature earns such models classification as a type of ‘seesaw’.

A lot of work has been done on the phenomenology of scalar triplets which, interestingly, also arise in left-right symmetric theories [1]. One can, however, still ask the question: is a single-triplet scenario self-sufficient, or does the replication of triplets (together with, say, the single scalar doublet of the SM) bring about any difference in phenomenology? This question, otherwise a purely academic one, acquires special meaning in the context of some neutrino mass models which aim to connect the mass ordering with the values of the mixing angles, thereby achieving some additional predictiveness. One class of such models depend on texture zeros, where a number of zero entries (usually restricted to two) in the mass matrix enable one to establish the desired connection. The existence of such zero entries require the imposition of some additional symmetry; it has, for example, been shown that a horizontal  $\mathcal{Z}_4$  symmetry can serve the purpose. The simultaneous requirement of zero textures and the type-II seesaw mechanism, however, turns out to be inconsistent, as has been discussed in earlier works [2]. The inconsistency is gone for two triplets. This resurrects the relevance of the phenomenology of two-triplet, one doublet scalar sectors, this time with practical implications. We have studied such phenomenology in reference [3]. An important conclusion of this study was that, whereas the doubly charged scalar in the single triplet scenario would decay mostly in the  $\ell^\pm \ell^\pm$  or  $W^\pm W^\pm$  modes, the decay channel  $H_1^{++} \rightarrow H_2^+ W^+$  acquires primacy over a large region of the parameter space. Some predictions on this in the context of the Large Hadron Collider were also shown in reference [3]. However, an added possibility with two triplet is the possibility of at least one CP-violating phase being there. This in principle can affect the phenomenology of the model, which is worth studying.

With this in view, we have analyzed here the one-doublet, two-triplet framework, including CP-violating effects arising via a relative phase between the triplets. Thus, the vev of one triplet has been made complex and consequently, the coefficient of the corresponding trilinear term in the scalar potential has also been rendered complex.

Indeed, the introduction of a phase results in some interesting findings that were not present when the relative phase was absent. First of all, as a result of mixing between two triplets and presence of a relative phase between them, something on which no phenomenological restrictions exists, the heavier doubly charged scalar can now decay frequently into the lighter doubly charged scalar plus the SM-like Higgs boson, i.e  $H_1^{++} \rightarrow H_2^{++} h$ , over a larger range of parameter space. This can give rise to a spectacular signal in the context of LHC. Basically, as a final state, we obtain  $H_1^{++} \rightarrow \ell^+ \ell^+ h$  i.e a doubly charged scalar decaying into two same-sign leptons plus the SM-like Higgs. This decay often dominates over all other

decay channels. When this decay is not present due to insufficient mass-difference between respective scalars, the decay  $H_2^{++} \rightarrow H_2^+ W^+$  mostly dominates, and its consequence was discussed in some detail in our earlier work [3] on the CP-conserving scenario.

Secondly, for some combination of parameters, the decays mentioned in the above paragraph are not possible with a vanishing or small phase, due to insufficient gap in masses between the respective scalars. However, if we continuously increase the value of the phase, keeping all the other parameters fixed, the mass difference between the scalars start in increase, so that the aforementioned channel finally opens up.

Thirdly, we have noticed in [3] that the gauge coupling dominated decay  $H_1^{++} \rightarrow H_2^+ W^+$  dominates over the Yukawa coupling dominated decay  $\Delta^{++} \rightarrow \ell^+ \ell^+$ , even in those region of parameter space where we have chosen the Yukawa coupling matrices to be sufficiently large ( $\simeq 1$ ). On the other hand, the CP-violating phase suppresses the neutrino mass matrix elements for the same value of the triplet vacuum expectation values (vev). This in turn requires an increase in the corresponding Yukawa coupling matrix elements, since the vev's and Yukawa couplings are related by the expression for neutrino masses. The outcome of this whole process is that, for several BPs, the decay  $H_1^{++} \rightarrow \ell^+ \ell^+$  competes with the decay into  $H_2^+ W^+$ .

Finally, the CP-conserving scenario marks out regions of the parameter space, where the branching ratios of the decays  $H_1^{++} \rightarrow \ell^+ \ell^+$  and  $H_1^{++} \rightarrow W^+ W^+$  are of comparable, though subdominant, rates. As the phase picks up, the same vev causes necessitates a hike in Yukawa coupling, as discussed above. In such situations, the decay  $H_1^{++} \rightarrow \ell^+ \ell^+$  mostly dominates over the  $W^+ W^+$  mode.

We present a summary of the scenario with a single triplet with complex vev on section 2. In section 3, we outline the two-triplet scenario with a complex phase, including the corresponding scalar potential. The composition of physical states, the benchmark points for our numerical study and the results are presented in section 4. We summarize and conclude in section 5.

## 2 A single scalar triplet with a CP-violating phase

We first give the reader a glimpse of the scenario with a single triplet  $\Delta = (\Delta^{++}, \Delta^+, \Delta^0)$ , over and above the usual Higgs doublet  $\phi$ , using the notation of [4].  $\Delta$  is equivalently denoted by the  $2 \times 2$  matrix

$$\Delta = \begin{pmatrix} \Delta^+ & \sqrt{2}\Delta^{++} \\ \sqrt{2}\Delta^0 & -\Delta^+ \end{pmatrix}. \quad (1)$$

The vev's of the doublet and the triplet are expressed as

$$\langle \phi \rangle_0 = \frac{1}{\sqrt{2}} \begin{pmatrix} 0 \\ v \end{pmatrix} \quad \text{and} \quad \langle \Delta \rangle_0 = \begin{pmatrix} 0 & 0 \\ v_T & 0 \end{pmatrix}, \quad (2)$$

respectively. The only doublet-dominated physical state that survives after the generation of gauge boson masses is a neutral scalar  $h$ .

The most general scalar potential including  $\phi$  and  $\Delta$  can be written as

$$\begin{aligned}
V(\phi, \Delta) = & a \phi^\dagger \phi + \frac{b}{2} \text{Tr}(\Delta^\dagger \Delta) + c(\phi^\dagger \phi)^2 + \frac{d}{4} (\text{Tr}(\Delta^\dagger \Delta))^2 \\
& + \frac{e-h}{2} \phi^\dagger \phi \text{Tr}(\Delta^\dagger \Delta) + \frac{f}{4} \text{Tr}(\Delta^\dagger \Delta^\dagger) \text{Tr}(\Delta \Delta) \\
& + h \phi^\dagger \Delta^\dagger \Delta \phi + \left( t \phi^\dagger \Delta \tilde{\phi} + \text{H.c.} \right), \tag{3}
\end{aligned}$$

where  $\tilde{\phi} \equiv i\tau_2 \phi^*$ . All parameters in the Higgs potential are real except  $t$  which is complex in general. By performing a global  $U(1)$  transformation,  $v$  can always be chosen real and positive. Because of the  $t$ -term in the potential there is no second global symmetry to make  $v_T$  real. Furthermore,  $t$  can also be complex and, therefore, it can be written as  $t = |t| e^{i\alpha}$  and  $v_T = w e^{i\gamma}$  with  $w \equiv |v_T|$ . Minimization of the scalar potential with respect to the phase of  $v_T$  i.e  $\gamma$ , gives the relation between the phases as  $\alpha + \gamma = \pi$ .<sup>1</sup>

The choice  $a < 0$ ,  $b > 0$  ensures that the dominant source of spontaneous symmetry breaking is the scalar doublet. It is further assumed, following [4], that

$$a, b \sim v^2; \quad c, d, e, f, h \sim 1; \quad |t| \ll v. \tag{4}$$

Such a choice is motivated by the following considerations

- The need to fulfill the electroweak symmetry breaking conditions,
- To have  $w \ll v$  sufficiently small, as required by the  $\rho$ -parameter constraint,
- To keep doublet-triplet mixing low in general, and
- To ensure that all quartic couplings are perturbative.

The mass terms for the singly-charged scalars can be expressed in a compact form as

$$\mathcal{L}_S^\pm = -(H^-, \phi^-) \mathcal{M}_+^2 \begin{pmatrix} H^+ \\ \phi^+ \end{pmatrix} \tag{5}$$

with

$$\mathcal{M}_+^2 = \begin{pmatrix} (q + h/2)v^2 & \sqrt{2}v(t^* - v_T h/2) \\ \sqrt{2}v(t - v_T^* h/2) & 2(q + h/2)w^2 \end{pmatrix} \quad \text{and} \quad q = \frac{|t|}{w}. \tag{6}$$

Keeping aside the charged Goldstone boson, the mass-squared of the singly-charged physical scalar is obtained as

$$m_{\Delta^+}^2 = \left( q + \frac{h}{2} \right) (v^2 + 2w^2), \tag{7}$$

while the doubly-charged scalar mass is expressed as

$$m_{\Delta^{++}}^2 = (h + q)v^2 + 2fw^2. \tag{8}$$

Thus, in the limit  $w \ll v$ ,

$$m_{\Delta^{++}}^2 - m_{\Delta^+}^2 \simeq \frac{h}{2}v^2. \tag{9}$$

Thus a substantial mass splitting between  $\Delta^{++}$  and  $\Delta^+$  is in general difficult. This tends to disfavour the  $\Delta^+ W^+$  decay channel of  $\Delta^{++}$ , as compared to  $\ell^+ \ell^+$  and  $W^+ W^+$ .

---

<sup>1</sup>For an analogous situation with two Higgs doublets, see, for example [5].

### 3 Two scalar triplets and a CP-violating phase

Strong evidence has accumulated in favour of neutrino oscillation from the solar, atmospheric, reactor and accelerator neutrino experiments over the last few years. It is now widely believed that neutrinos have non-degenerate masses and a very characteristic mixing pattern. A lot, however, is yet to be known, including the mass generation mechanism and the absolute values of the masses, as opposed to mass-squared differences which affect oscillation rates. Also, a lot of effort is on to ascertain the nature of neutrino mass hierarchy, including the signs of the mass-squared differences. A gateway to information of the above kinds is the light neutrino mass matrix, in a basis where the charged lepton mass matrix is diagonal.

Here, too, in the absence of very clear guidelines, various ‘textures’ for the neutrino mass matrix are often investigated. A possibility that frequently enters into such investigations is one where the mass matrix has some zero entries, perhaps as the consequence of some built-in symmetry of lepton flavours. At the same time, such ‘zero textures’ lead to a higher degree of predictiveness and inter-relation between mass eigenvalues and mixing angles, by virtue of having fewer free parameters, see for example [6]. In the context of Majorana neutrinos which have a symmetric mass matrix, various texture zeros have thus been studied from a number of angles. Of them, two-zero textures have a rather wide acceptability.

It has been shown in [7] that none of the seven possible two-zero-texture cases can be achieved by assuming only one scalar triplet. However, this is not the case with two triplets, where several of the seven possible two-zero textures are allowed. Therefore, it is important to examine the phenomenological consequences of an augmented triplet sector, if Type-II seesaw has to be consistent with the texture-zero approach.

One is thus encouraged to consider a scenario consisting of one complex doublet and two  $Y = 2$  triplet scalars  $\Delta_1, \Delta_2$ , both written as  $2 \times 2$  matrices:

$$\Delta_1 = \begin{pmatrix} \delta_1^+ & \sqrt{2}\delta_1^{++} \\ \sqrt{2}\delta_1^0 & -\delta_1^+ \end{pmatrix} \quad \text{and} \quad \Delta_2 = \begin{pmatrix} \delta_2^+ & \sqrt{2}\delta_2^{++} \\ \sqrt{2}\delta_2^0 & -\delta_2^+ \end{pmatrix}. \quad (10)$$

The vev’s of the scalar triplets are given by

$$\langle \Delta_1 \rangle_0 = \begin{pmatrix} 0 & 0 \\ w_1 & 0 \end{pmatrix} \quad \text{and} \quad \langle \Delta_2 \rangle_0 = \begin{pmatrix} 0 & 0 \\ w_2 & 0 \end{pmatrix}. \quad (11)$$

The vev of the Higgs doublet is as usual given by equation (2).

The scalar potential in this model involving  $\phi, \Delta_1$  and  $\Delta_2$  can be written as

$$\begin{aligned} V(\phi, \Delta_1, \Delta_2) = & \\ & a \phi^\dagger \phi + \frac{1}{2} b_{kl} \text{Tr} (\Delta_k^\dagger \Delta_l) + c(\phi^\dagger \phi)^2 + \frac{1}{4} d_{kl} \left( \text{Tr} (\Delta_k^\dagger \Delta_l) \right)^2 \\ & + \frac{1}{2} (e_{kl} - h_{kl}) \phi^\dagger \phi \text{Tr} (\Delta_k^\dagger \Delta_l) + \frac{1}{4} f_{kl} \text{Tr} (\Delta_k^\dagger \Delta_l^\dagger) \text{Tr} (\Delta_k \Delta_l) \\ & + h_{kl} \phi^\dagger \Delta_k^\dagger \Delta_l \phi + g \text{Tr} (\Delta_1^\dagger \Delta_2) \text{Tr} (\Delta_2^\dagger \Delta_1) + g' \text{Tr} (\Delta_1^\dagger \Delta_1) \text{Tr} (\Delta_2^\dagger \Delta_2) \\ & + \left( t_k \phi^\dagger \Delta_k \tilde{\phi} + \text{H.c.} \right), \end{aligned} \quad (12)$$

where summation over  $k, l = 1, 2$  is understood. This potential is not the most general one, since we neglected some of the quartic terms. This is justified in view of the scope of this paper, as laid out in the introduction.

In [3], all the vev's as well the parameters in the potential were assumed to be real. As has already been mentioned, this need not be the situation in general. To see the phenomenology including CP-violation, we make a minimal extension of the simplified scenario by postulating *one* CP-violating phase to exist. This entails a complex vev for any one triplet (in our case we have chosen it to be  $\Delta_1$ ). At the same time, there is a complex phase in the coefficient  $t_1$  of the trilinear term in the potential. Thus one can write  $t_1 = |t_1| e^{i\beta}$  and  $w_1 = |w_1| e^{i\alpha}$ .

Using considerations very similar to those for the single-triplet model, we have taken

$$a, b_{kl} \sim v^2; \quad c, d_{kl}, e_{kl}, h_{kl}, f_{kl}, g, g' \sim 1; \quad |t_k| \ll v. \quad (13)$$

We also chosen to restrict ourselves to cases where  $w_1, w_2 \ll v$ , keeping in mind the constraint on the  $\rho$ -parameter.

The mass eigenvalues, scalar mixing matrices etc. following from the potential (12) can only be obtained numerically in general. However, one can use the smallness of the triplet vev's  $w_k$ , and drop the quartic terms in the scalar triplets during the diagonalisation of the mass matrices. This enables one to use approximate analytical expressions, which makes our broad conclusions somewhat transparent. However, the numerical results presented in section 4 are obtained using the full potential (12), including the effects of the triplet vev's.

It is convenient to speak in terms of the following matrices and vectors:

$$B = (b_{kl}), \quad E = (e_{kl}), \quad H = (h_{kl}), \quad (14)$$

$$t = \begin{pmatrix} |t_1| \cos \beta \\ t_2 \end{pmatrix}, \quad t' = \begin{pmatrix} |t_1| \sin \beta \\ 0 \end{pmatrix}, \quad w = \begin{pmatrix} |w_1| \cos \alpha \\ w_2 \end{pmatrix}, \quad w' = \begin{pmatrix} |w_1| \sin \alpha \\ 0 \end{pmatrix}. \quad (15)$$

In terms of them, the conditions for a stationary point of the potential are

$$\left( B + \frac{v^2}{2} (E - H) \right) w + v^2 t = 0, \quad (16)$$

$$a + cv^2 + \frac{1}{2} w^T (E - H) w + 2t \cdot w + 2t' \cdot w' + \frac{1}{2} w'^T (E - H) w' = 0, \quad (17)$$

$$\left( b_{11} + \frac{v^2}{2} (e_{11} - h_{11}) \right) |w_1| \sin \alpha - v^2 |t_1| \sin \beta = 0, \quad (18)$$

using the notation  $t \cdot w = \sum_k t_k w_k$ . These three equations are exact if one neglects all terms quartic in the triplet vev's in  $V_0 \equiv V(\langle \phi \rangle_0, \langle \Delta \rangle_0)$ . In equation (17) we have already divided by  $v$ , assuming  $v \neq 0$ . The small vev's  $w_k$  are thereafter obtained as

$$w = -v^2 \left( B + \frac{1}{2} v^2 (E - H) \right)^{-1} t. \quad (19)$$

And from equation (18) the phase of  $t_1$  can be expressed as

$$\sin \beta = \frac{v^{-2} (b_{11} + \frac{v^2}{2} (e_{11} - h_{11})) |w_1| \sin \alpha}{|t_1|} \quad (20)$$

This re-iterates the fact that the phases  $t_1$  and  $w_1$  are related to each other. It is also evident from (20) that the value of the angle  $\alpha$  has to be  $n\pi$  where  $n = 0, 1, 2, 3, \dots$  when the phase  $\beta$  is absent.

We next discuss the mass matrices of charged scalars. The mass matrix of the doubly-charged scalars is obtained as

$$\mathcal{M}_{++}^2 = B + \frac{v^2}{2} (E + H). \quad (21)$$

It is interesting to note that if we drop those quartic terms for simplification from our scalar potential, then our doubly charged mass matrix remains the same as in [3]. This gives the impression that the relative phase between triplets does not affect the doubly charged mass matrix if we drop the quartic terms in the potential. But in our numerical calculation, where we have taken the full scalar potential including the quartic terms, we find such a dependence, arising obviously from the quartic terms. This will be discussed further in the next section.

As for the singly-charged fields  $\Delta_k^+$ , one has consider their mixing with  $\phi^+$  of the Higgs doublet. and This introduces the CP-violating phase into the singly charged mass matrix. We write the mass term as

$$- \mathcal{L}_S^\pm = (\delta_1^-, \delta_2^-, \phi^-) \mathcal{M}_+^2 \begin{pmatrix} \delta_1^+ \\ \delta_2^+ \\ \phi^+ \end{pmatrix} + \text{H.c.}, \quad (22)$$

equation (12) leads to

$$\mathcal{M}_+^2 = \begin{pmatrix} B + \frac{v^2}{2} E & \sqrt{2}v(t - Hw/2) \\ \sqrt{2}v(t - Hw/2)^\dagger & a + cv^2 + \frac{1}{2}w^T(E + H)w + \frac{1}{2}w'^T(E + H)w' \end{pmatrix}. \quad (23)$$

Now, this mass matrix must have a zero eigenvalue, corresponding to the would-be-Goldstone boson. Indeed, on substituting the minimization equations (16), (17) and (18), we see that

$$\text{Det}(\mathcal{M}_+^2) = 0, \quad (24)$$

which ensures a consistency check.

The mass matrices (22) and (23) are diagonalized by

$$U_1^\dagger \mathcal{M}_{++}^2 U_1 = \text{diag}(M_1^2, M_2^2) \quad \text{and} \quad U_2^\dagger \mathcal{M}_+^2 U_2 = \text{diag}(\mu_1^2, \mu_2^2, 0), \quad (25)$$

respectively, with

$$\begin{pmatrix} \delta_1^{++} \\ \delta_2^{++} \end{pmatrix} = U_1 \begin{pmatrix} H_1^{++} \\ H_2^{++} \end{pmatrix}, \quad \begin{pmatrix} \delta_1^+ \\ \delta_2^+ \\ \phi^+ \end{pmatrix} = U_2 \begin{pmatrix} H_1^+ \\ H_2^+ \\ G^+ \end{pmatrix}. \quad (26)$$

We have denoted the fields with definite mass by  $H_k^{++}$  and  $H_k^+$ , and  $G^+$  is the charged would-be-Goldstone boson.

We also outline the neutral sector of the model, which cannot now be separated into CP-even and CP-odd sectors. Thus the mass matrix for the neutral sector of the present scenario turns out to be a  $6 \times 6$  matrix, including mixing between real and imaginary parts of the complex neutral fields. The symmetric neutral mass matrix is denoted by  $\mathcal{M}_{neut}$ , whose elements are listed in the Appendix. So, the mass term for the neutral part can be written as :

$$- \mathcal{L}_S^0 = (N_{01}, N_{02}, N_{03}, N_{04}, N_{05}, N_{06}) \mathcal{M}_{neut}^2 \begin{pmatrix} N_{01} \\ N_{02} \\ N_{03} \\ N_{04} \\ N_{05} \\ N_{06} \end{pmatrix} + \text{H.c.}, \quad (27)$$

Where  $N_{0n}$  s are the neutral states in flavor basis. This mass matrix is diagonalized by

$$U_3^\dagger \mathcal{M}_{neut}^2 U_3 = \text{diag} (M_{01}^2, M_{02}^2, M_{03}^2, M_{04}^2, M_h^2, 0) \quad (28)$$

with

$$\begin{pmatrix} N_{01} \\ N_{02} \\ N_{03} \\ N_{04} \\ N_{05} \\ N_{06} \end{pmatrix} = U_3 \begin{pmatrix} H_{01} \\ H_{02} \\ H_{03} \\ H_{04} \\ h \\ G_0 \end{pmatrix}. \quad (29)$$

Where  $h$  is identified with the Standard Model Higgs boson and  $G_0$  is the neutral Goldstone boson.

It is interesting to note that once we remove the phases of coefficient of trilinear term in scalar potential and the vev of triplet  $H_1^{++}$  by setting  $\alpha = \beta = 0$ , then the mixing between the CP-even and CP-odd scalars vanishes and we get back the usual separate  $3 \times 3$  matrices for these two sectors. This also serves as a consistency check for the model. And ofcourse the lightest neutral scalar of this sector can be identified with SM Higgs.

The  $\Delta L = 2$  Yukawa interactions of the triplets are

$$\mathcal{L}_Y = \frac{1}{2} \sum_{k=1}^2 y_{ij}^{(k)} L_i^T C^{-1} i\tau_2 \Delta_k L_j + \text{H.c.}, \quad (30)$$

where  $C$  is the charge conjugation matrix, the  $y_{ij}^{(k)}$  are the symmetric Yukawa coupling matrices of the triplets  $\Delta_k$ , and the  $i, j$  are the summation indices over the three neutrino flavours. The charged-lepton mass matrix is diagonal in this basis.

The neutrino mass matrix is generated from  $\mathcal{L}_Y$  as

$$(M_\nu)_{ij} = y_{ij}^{(1)} |w_1| \cos\alpha + y_{ij}^{(2)} w_2. \quad (31)$$

This relates the Yukawa coupling constants  $y_{ij}^{(1)}$ ,  $y_{ij}^{(2)}$  and the real part of the triplet vev's, namely,  $|w_1| \cos\alpha$  and  $w_2$ .



The neutrino mass eigenvalues are fixed according to a particular type of mass spectrum. In this work we illustrate our points, without any loss of generality, in the context of normal hierarchy, setting the lowest neutrino mass eigenvalue to zero. Next, using the observed central values of the various lepton mixing angles, the elements of the neutrino mass matrix  $M_\nu$  can be found by using

$$M_\nu = U^\dagger \hat{M}_\nu U, \quad (32)$$

where  $U$  is the PMNS matrix given by [8]

$$U = \begin{pmatrix} c_{12}c_{13} & s_{12}c_{13} & s_{13}e^{-i\delta} \\ -s_{12}c_{23} - c_{12}s_{23}s_{13}e^{i\delta} & c_{12}c_{23} - s_{12}s_{23}s_{13}e^{i\delta} & s_{23}c_{13} \\ s_{12}s_{23} - c_{12}c_{23}s_{13}e^{i\delta} & -c_{12}s_{23} - s_{12}c_{23}s_{13}e^{i\delta} & c_{23}c_{13} \end{pmatrix} \quad (33)$$

and  $\hat{M}_\nu$  is the diagonal matrix of the neutrino masses. We have neglected possible Majorana phases, and the recent global analysis of neutrino data are used to compute the elements of  $U$  [9]. Also, the phase  $\delta$  has been set to zero. For  $\theta_{13}$ , the results from the Daya Bay and RENO experiments [10, 11] have been used.

After all this, all terms of the left-hand side of equation (30) are approximately known, which is sufficient for predicting phenomenology in the 100 GeV - 1 TeV scale. The actual mass matrix thus constructed, on numerical evaluation, approximately reflects a two-zero texture which is one of the motivations of this study.

For each benchmark point used in the next section,  $w_1$  and  $w_2$  get determined by values of the other parameters in the scalar potential. Of course, the coupling matrices  $y^{(1)}$  and  $y^{(2)}$  are still indeterminate. We fix the matrix  $y^{(2)}$  by choosing a single suitable value for all elements of the  $\mu$ - $\tau$  block and a smaller value for the rest of the matrix. As has already been mentioned in [3], our broad conclusions do not depend on this ‘working rule’.

## 4 Benchmark points and numerical predictions

The trademark signal of Higgs triplets is contained in the doubly charged components. In the current scenario, too, one would like to see the signatures of the two doubly charged scalars, especially the heavier one, namely  $H_1^{++}$  whose decays have already been shown to contain a rather rich phenomenology.

The  $H_1^{++}$ , produced at the LHC via the Drell-Yan process, can in general have two-body decays in the following channels:

$$H_1^{++} \rightarrow H_2^{++}h, \quad (34)$$

$$H_1^{++} \rightarrow \ell_i^+ \ell_j^+, \quad (35)$$

$$H_1^{++} \rightarrow W^+W^+, \quad (36)$$

$$H_1^{++} \rightarrow H_2^+W^+, \quad (37)$$

$$H_2^{++} \rightarrow \ell_i^+ \ell_j^+, \quad (38)$$

$$H_2^{++} \rightarrow W^+W^+, \quad (39)$$

with  $h$  is the SM-like Higgs and  $\ell_i, \ell_j = e, \mu$ .

The decay modes (34) and (37) are absent in the single-triplet model. On the other hand, mixing between two triplets opens up situations where the mass separation between  $H_1^{++}, H_2^{++}$  and  $H_1^{++}, H_2^+$  is sufficient to kinematically allow the transitions (34) and (37). The decay (34) opens up a spectacular signal, especially when  $H_2^{++}$  mostly decays into two same sign leptons, leading to

$$H_1^{++} \rightarrow \ell_i^+ \ell_j^+ h \quad (40)$$

Let us denote the mass of SM Higgs by  $M_h$ , that of  $H_k^{++}$  by  $M_k$  and that of  $H_k^+$  by  $\mu_k$  ( $k = 1, 2$ ). Then, in the convention  $M_1 > M_2$ ,  $\mu_1 > \mu_2$ , the decays (34) and (37) are possible only if  $M_1 > M_2 + M_h$  and  $M_1 > \mu_2 + m_W$ . We demonstrate numerically that this can naturally happen, by considering three distinct regions of the parameter space and selecting four benchmark points (BPs) for each region. The relative phase between two triplets also plays an important role in these cases. In order to emphasise this, we have also chosen three different values of the phase, namely  $\alpha = 30^\circ, 45^\circ$  and  $60^\circ$  for each benchmark point. Thus we have considered 36 BPs altogether, comprising three distinct regions of the parameter space and relative phases between triplets to justify our findings.

We have seen that, in a single-triplet model, the doubly-charged Higgs decays into either  $\ell_i^+ \ell_j^+$  or  $W^+ W^+$ . The former is controlled by the  $\Delta L = 2$  Yukawa couplings  $y_{ij}$ , while the latter is driven by  $w$ , the triplet vev. Neutrino masses are given by (31), implying large values of  $y_{ij}$  for small  $w$ , and vice versa. Interestingly, the presence of triplet phase through the  $\cos\alpha$  term in this equation actually suppresses the vev  $w_1$  of the first triplet. This in turn implies that we get higher values for Yukawa coupling matrix entries  $y_1^{ij}$  compared to the case where CP-violating effects are absent. Accordingly, we have identified, for the chosen values of triplet phase, three regions in the parameter space, corresponding to

- i)  $\Gamma(H_{1,2}^{++} \rightarrow \ell_i^+ \ell_j^+) \ll \Gamma(H_{1,2}^{++} \rightarrow W^+ W^+)$ ,
- ii)  $\Gamma(H_{1,2}^{++} \rightarrow \ell_i^+ \ell_j^+) \gg \Gamma(H_{1,2}^{++} \rightarrow W^+ W^+)$ ,
- iii)  $\Gamma(H_{1,2}^{++} \rightarrow \ell_i^+ \ell_j^+) \sim \Gamma(H_{1,2}^{++} \rightarrow W^+ W^+)$ .

These are referred to as scenarios 1, 2 and 3 respectively in the subsequent discussion.

The masses of the various physical state scalars are shown in Tables. Although our study involves mainly the phenomenology of charged scalars, we have also listed the masses of neutral scalars. It should be noted that the lightest neutral scalar, dominated by the doublet component, has mass  $\sim 125$  GeV for each BP, identifying it with the observed Higgs particle.

One also notices a rather interesting effect of the triplet phase, shown in Figures (1a) and (1b). In Figure (1a) we have plotted the variation of mass difference between  $H_1^{++}$  and  $H_2^{++}$  with respect to variation of the phase  $\alpha$ . The mass difference between  $H_1^{++}$  and  $H_2^+$  is similarly presented in Figure (1b). If the mass differences do not allow the decays (34) and (37) for  $\alpha = 0$ , they open up with increase in the phase of the triplet, when all other parameters are at fixed values.

Earlier, we neglected contributions from the quartic terms in our scalar potential in the approximate forms of the doubly- and singly-charged mass matrices. However, the import of the phase is not properly captured unless one retains these terms. Thus it is only via a full

numerical analysis of the potential retaining all terms that the above effect of the phase of the trilinear term becomes apparent.

It should also be noted that the cosine of the complex phase suppresses the contribution to neutrino masses. Consequently, for the same triplet vev, one requires larger values of the Yukawa interaction strengths. This makes the  $l^+l^+$  decay mode of a doubly charged scalar more competitive with  $W^+W^+$ , as compared to the results in ([3]).

The branching ratios for a given scalar in different channels are of course dependent on the various parameters that characterise a BP. We list all the charged scalar masses in Tables 1, 4 and 7. Moreover, the neutral scalar masses are shown in Tables 2, 5 and 8 for three different values of triplet phase  $\alpha$ . The branching ratios for  $H_1^{++}$  and  $H_2^{++}$  for different triplet phases are listed in Tables 3,6 and 9, together with their pair-production cross sections at the LHC with  $\sqrt{s} = 13$  TeV. The cross sections and branching ratios have been calculated with the help of the package FeynRules (version 1.6.0) [12, 13], thus creating a new UFO model file in MadGraph5-aMC@NLO (version 2.3.3) [14]. Using the full machinery of scalar mixing in this model, the decay widths into various channels have been obtained.

The presence of the phase  $\alpha$  also affects phenomenology in the following way. Suppose, in the absence of any additional symmetry in hierarchy, the matrices  $B$ ,  $E$  and  $H$  are such that the resulting elements of each charged mass matrix are of similar order. This would normally result in rather low mass-splitting between  $H_1^{++}$  and  $H_2^{++}$ , so long as the CP-violating phase is vanishing or small. For large  $\alpha$ , however, the degree of doublet-triplet mixing will be different for the two triplets. The splitting between  $H_1^{++}$  and  $H_2^{++}$  consequently goes up and the decay  $H_1^{++} \rightarrow H_2^{++}h$  tends to dominate. Drell-Yan pair production of  $H_1^{\pm\pm}$  is  $hl^\pm\ell^\pm$ , i.e an invariant mass peak in same-sign dileptons, together with an SM-like Higgs, that can be identified in the usual search channels at the LHC.

From Tables 3, 6 and 9, we see that decay (40) dominates, when the masses of  $H_1^{++}$  and  $H_2^{++}$  are sufficiently separated. Also, when the phase space needed for this decay (40) is not available, the process (37) dominates over all other remaining decays. Benchmark points when decay (37) mostly dominates for  $H_1^{\pm\pm}$  have been discussed in detail in reference [3]. Here we supplement those observations with some results for the case when decay (40) has an interesting consequence, as exemplified by Figures 2 and 3.

Figure 2 specifically shows the effect of CP-violating phase going up. We have seen in Figure 1 that the mass difference between  $H_1^{++}$  and  $H_2^{++}$  undergoes significant enhancement if, with other parameters unchanged, once the phase  $\alpha$  is increased beyond  $60^\circ$ , the decay  $H_1^{++} \rightarrow H_2^{++}h$  not only opens up but also becomes dominant. This point is accumulated in Figure 2, for which the choice of parameters is detailed in the caption. We simulated the same-sign dilepton final states and notice that there are two invariant mass peaks for  $\alpha = 60^\circ$  in BP 4 of Scenario 2, as shown in Figure (2a). However, Figure (2b) shows only one peak for  $\alpha = 65^\circ$ , for which mass of  $H_2^{++}$  remains practically the same. The increase in the CP-violating phase raises mass of  $H_1^{++}$  and causes decay (40) to be overwhelmingly dominant. The two invariant mass peaks consequently make way for a single one at  $M_{H_2^{++}}$ . The identification of SM-like Higgs along with the same-sign dilepton peak can be an interesting signature of such a situation.

Figure 3 captures BP's, for which decay (37) is not overwhelmingly dominant. There, in addition to decay (37), process (35), too has non-negligible branching ratios. For such situations, we have simulated the same-sign dilepton final states from both  $H_1^{\pm\pm}$  and  $H_2^{\pm\pm}$ .

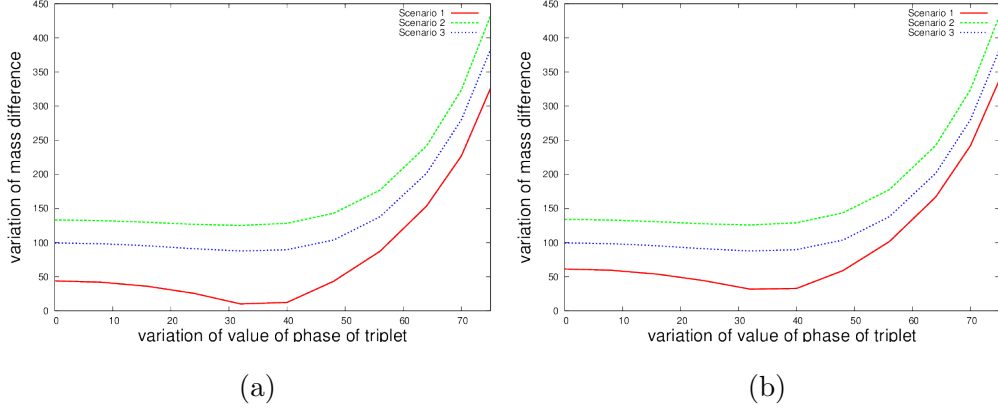


Figure 1: Variation of mass difference between (a)  $\mathcal{H}_1^{++}$  and  $\mathcal{H}_2^{++}$  and (b)  $\mathcal{H}_1^{++}$  and  $\mathcal{H}_2^+$  with phase of triplet  $\alpha$

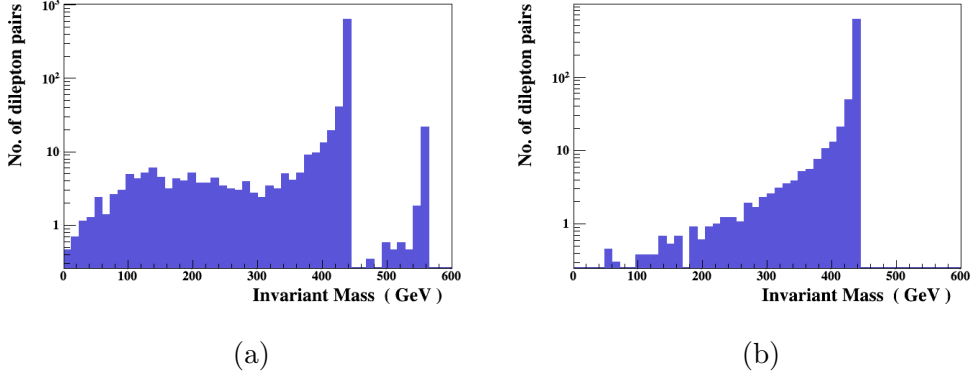
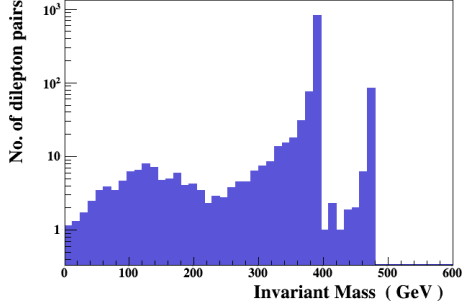
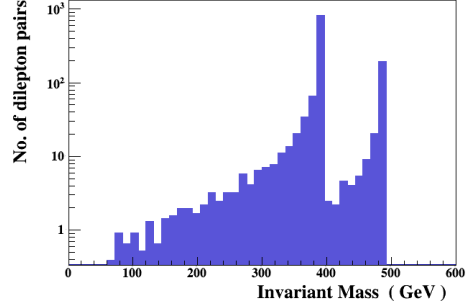


Figure 2: Invariant mass distribution of same sign di-leptons for (a)  $\alpha = 60^\circ$  and (b)  $\alpha = 65^\circ$  for BP 4 of Scenario 2

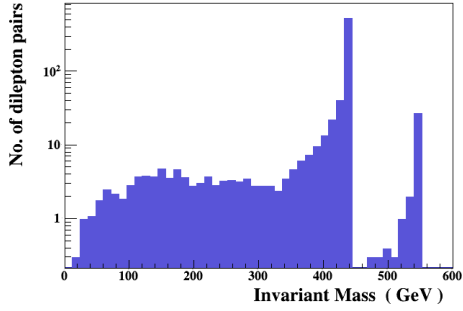
The leptons selected for this purpose satisfy:  $|p_T^{\text{lepton}}| > 20 \text{ GeV}$ ,  $|\eta_{\text{lep}}| < 2.5$ ,  $|\Delta R_{\ell\ell}| < 0.2$  and  $|\Delta R_{\ell j}| < 0.4$  where  $\Delta R^2 = \Delta\eta^2 + \Delta\phi^2$ . The two invariant mass peaks in each of the plots in Figure 3, bear testimony to the existence of two doubly-charged scalar states decaying in the dilepton channel.



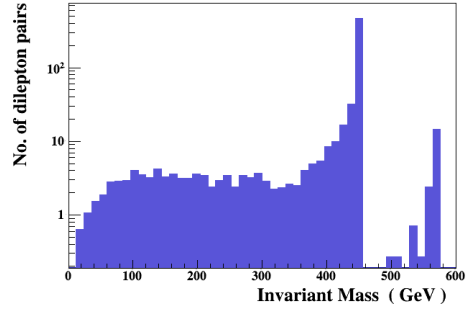
(a)



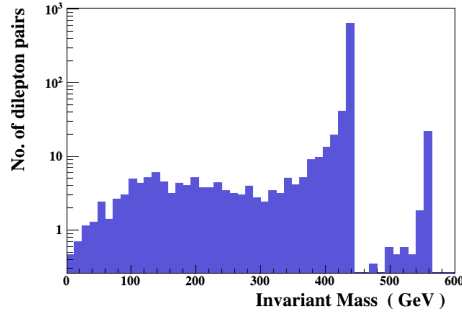
(b)



(c)



(d)



(e)

Figure 3: Invariant mass distribution of same sign di-leptons for chosen benchmark points. In (a) BP 3 and (b) BP 4 of Scenario 2 for  $\alpha = 30^\circ$ . In (c) BP 3 and (d) BP 4 of Scenario 2 for  $\alpha = 45^\circ$ . In (e) BP 4 of Scenario 2 for  $\alpha = 60^\circ$

$\alpha = 30^\circ$	Mass (GeV)	BP 1	BP 2	BP 3	BP 4
Scenario 1	$H_1^{++}$	516.61	513.83	522.13	537.62
	$H_2^{++}$	391.40	389.82	426.93	440.96
	$H_1^+$	516.58	513.81	522.10	537.55
	$H_2^+$	390.60	389.79	408.83	416.30
Scenario 2	$H_1^{++}$	526.00	529.85	477.38	485.76
	$H_2^{++}$	397.61	390.10	389.10	389.33
	$H_1^+$	525.94	529.80	477.34	485.70
	$H_2^+$	393.79	390.01	389.00	389.28
Scenario 3	$H_1^{++}$	558.71	562.35	485.76	477.38
	$H_2^{++}$	427.00	407.20	389.33	389.10
	$H_1^+$	557.59	559.11	485.70	477.34
	$H_2^+$	392.90	405.91	389.28	389.00

Table 1: Charged scalar masses for phase  $\alpha = 30^\circ$ .

$\alpha = 30^\circ$	Mass (GeV)	BP 1	BP 2	BP 3	BP 4
Scenario 1	$H_{01}$	730.57	726.65	738.36	760.19
	$H_{02}$	730.49	726.62	738.32	760.15
	$H_{03}$	552.30	551.25	551.40	552.65
	$H_{04}$	552.15	551.20	551.34	552.56
	$h$	125.16	125.18	125.20	125.15
Scenario 2	$H_{01}$	743.85	749.33	675.11	686.96
	$H_{02}$	743.00	749.25	675.00	686.90
	$H_{03}$	552.21	551.50	550.17	550.53
	$H_{04}$	552.10	551.39	550.05	550.40
	$h$	125.21	125.18	125.22	125.23
Scenario 3	$H_{01}$	787.10	789.25	687.00	676.15
	$H_{02}$	787.00	789.10	686.90	676.08
	$H_{03}$	541.16	542.00	552.21	549.90
	$H_{04}$	541.07	541.91	552.00	549.75
	$h$	125.23	125.26	125.13	125.16

Table 2: Neutral scalar masses for phase  $\alpha = 30^\circ$ .

$\alpha = 30^\circ$	Data	BP 1	BP 2	BP 3	BP 4
Scenario 1	$\text{BR}(H_1^{++} \rightarrow H_2^{++}h)$	$5.1 \times 10^{-3}$	not allowed	not allowed	not allowed
	$\text{BR}(H_1^{++} \rightarrow H_2^+W^+)$	0.99	0.99	0.79	0.99
	$\text{BR}(H_1^{++} \rightarrow W^+W^+)$	$2.8 \times 10^{-3}$	$6.5 \times 10^{-2}$	0.21	$3.1 \times 10^{-7}$
	$\text{BR}(H_1^{++} \rightarrow \ell_i^+ \ell_j^+)$	$4.8 \times 10^{-21}$	$1.6 \times 10^{-20}$	$1.3 \times 10^{-18}$	$2.1 \times 10^{-23}$
	$\text{BR}(H_2^{++} \rightarrow W^+W^+)$	0.99	0.99	0.99	0.99
	$\text{BR}(H_2^{++} \rightarrow \ell_i^+ \ell_j^+)$	$1.6 \times 10^{-18}$	$2.7 \times 10^{-18}$	$3.9 \times 10^{-17}$	$1.3 \times 10^{-20}$
	$\sigma(pp \rightarrow H_1^{++}H_1^{--})$	1.10 fb	1.13 fb	1.05 fb	0.42 fb
	$\sigma(pp \rightarrow H_2^{++}H_2^{--})$	3.97 fb	4.10 fb	2.70 fb	1.06 fb
Scenario 2	$\text{BR}(H_1^{++} \rightarrow H_2^{++}h)$	0.84	0.96	not allowed	not allowed
	$\text{BR}(H_1^{++} \rightarrow H_2^+W^+)$	0.13	0.03	0.76	0.42
	$\text{BR}(H_1^{++} \rightarrow W^+W^+)$	$3.1 \times 10^{-20}$	$1.9 \times 10^{-20}$	$1.2 \times 10^{-19}$	$2.8 \times 10^{-21}$
	$\text{BR}(H_1^{++} \rightarrow \ell_i^+ \ell_j^+)$	0.03	$8.9 \times 10^{-3}$	0.24	0.58
	$\text{BR}(H_2^{++} \rightarrow W^+W^+)$	$1.9 \times 10^{-19}$	$2.8 \times 10^{-19}$	$1.8 \times 10^{-20}$	$3.7 \times 10^{-19}$
	$\text{BR}(H_2^{++} \rightarrow \ell_i^+ \ell_j^+)$	0.99	0.99	0.99	0.99
	$\sigma(pp \rightarrow H_1^{++}H_1^{--})$	1.01 fb	1.02 fb	1.56 fb	1.43 fb
	$\sigma(pp \rightarrow H_2^{++}H_2^{--})$	3.60 fb	4.04 fb	3.97 fb	3.95 fb
Scenario 3	$\text{BR}(H_1^{++} \rightarrow H_2^{++}h)$	0.99	0.99	not allowed	not allowed
	$\text{BR}(H_1^{++} \rightarrow H_2^+W^+)$	$2.1 \times 10^{-3}$	$1.3 \times 10^{-2}$	0.99	0.99
	$\text{BR}(H_1^{++} \rightarrow W^+W^+)$	$2.6 \times 10^{-14}$	$3.1 \times 10^{-14}$	$4.3 \times 10^{-10}$	$2.8 \times 10^{-11}$
	$\text{BR}(H_1^{++} \rightarrow \ell_i^+ \ell_j^+)$	$1.5 \times 10^{-11}$	$2.3 \times 10^{-11}$	$3.7 \times 10^{-7}$	$5.4 \times 10^{-8}$
	$\text{BR}(H_2^{++} \rightarrow W^+W^+)$	0.03	0.01	0.04	0.02
	$\text{BR}(H_2^{++} \rightarrow \ell_i^+ \ell_j^+)$	0.97	0.99	0.96	0.98
	$\sigma(pp \rightarrow H_1^{++}H_1^{--})$	0.77 fb	0.74 fb	1.45 fb	1.58 fb
	$\sigma(pp \rightarrow H_2^{++}H_2^{--})$	3.61 fb	2.75 fb	3.95 fb	3.98 fb

Table 3: Decay branching ratios and production cross sections for doubly-charged scalars for phase  $\alpha = 30^\circ$ .



$\alpha = 45^\circ$	Mass (GeV)	BP 1	BP 2	BP 3	BP 4
Scenario 1	$H_1^{++}$	542.27	539.35	549.85	566.55
	$H_2^{++}$	406.60	405.20	438.46	450.96
	$H_1^+$	542.22	539.20	548.73	564.92
	$H_2^+$	405.90	405.07	422.28	428.94
Scenario 2	$H_1^{++}$	543.30	538.15	551.62	564.34
	$H_2^{++}$	405.10	404.10	440.10	448.82
	$H_1^+$	542.50	537.65	550.90	563.65
	$H_2^+$	405.00	403.20	439.72	447.90
Scenario 3	$H_1^{++}$	545.82	540.32	550.90	567.80
	$H_2^{++}$	409.80	405.00	439.50	452.45
	$H_1^+$	544.71	539.46	550.15	565.90
	$H_2^+$	409.00	404.75	425.38	432.80

Table 4: Charged scalar masses for phase  $\alpha = 45^\circ$ .

$\alpha = 45^\circ$	Mass (GeV)	BP 1	BP 2	BP 3	BP 4
Scenario 1	$H_{01}$	766.78	762.75	774.79	797.22
	$H_{02}$	766.60	762.11	774.23	797.00
	$H_{03}$	573.00	572.50	575.50	576.17
	$H_{04}$	572.65	572.00	575.15	575.95
	$h$	125.15	125.22	125.19	125.13
Scenario 2	$H_{01}$	768.10	760.37	772.90	795.85
	$H_{02}$	768.00	760.13	772.75	795.50
	$H_{03}$	575.32	570.00	574.30	576.85
	$H_{04}$	575.15	569.22	573.78	576.20
	$h$	125.12	125.16	125.24	125.17
Scenario 3	$H_{01}$	771.10	758.52	778.10	798.37
	$H_{02}$	770.85	758.00	777.85	798.00
	$H_{03}$	577.31	568.75	578.29	577.21
	$H_{04}$	577.00	568.13	578.00	577.00
	$h$	125.18	125.21	125.13	125.16

Table 5: Neutral scalar masses for phase  $\alpha = 45^\circ$ .

$\alpha = 45^\circ$	Data	BP 1	BP 2	BP 3	BP 4
Scenario 1	$\text{BR}(H_1^{++} \rightarrow H_2^{++}h)$	0.99	0.99	not allowed	not allowed
	$\text{BR}(H_1^{++} \rightarrow H_2^+W^+)$	$8.2 \times 10^{-4}$	$9.1 \times 10^{-4}$	0.90	0.96
	$\text{BR}(H_1^{++} \rightarrow W^+W^+)$	$2.4 \times 10^{-5}$	$1.7 \times 10^{-4}$	0.09	0.04
	$\text{BR}(H_1^{++} \rightarrow \ell_i^+ \ell_j^+)$	$3.1 \times 10^{-22}$	$3.8 \times 10^{-22}$	$6.1 \times 10^{-19}$	$4.2 \times 10^{-20}$
	$\text{BR}(H_2^{++} \rightarrow W^+W^+)$	0.99	0.99	0.99	0.99
	$\text{BR}(H_2^{++} \rightarrow \ell_i^+ \ell_j^+)$	$7.4 \times 10^{-19}$	$8.3 \times 10^{-19}$	$2.1 \times 10^{-19}$	$6.7 \times 10^{-19}$
	$\sigma(pp \rightarrow H_1^{++}H_1^{--})$	0.88 fb	0.87 fb	0.80 fb	0.71 fb
	$\sigma(pp \rightarrow H_2^{++}H_2^{--})$	3.39 fb	3.33 fb	2.43 fb	2.13 fb
Scenario 2	$\text{BR}(H_1^{++} \rightarrow H_2^{++}h)$	0.99	0.99	not allowed	not allowed
	$\text{BR}(H_1^{++} \rightarrow H_2^+W^+)$	$4.5 \times 10^{-4}$	$3.9 \times 10^{-4}$	0.64	0.88
	$\text{BR}(H_1^{++} \rightarrow W^+W^+)$	$1.3 \times 10^{-21}$	$9.1 \times 10^{-22}$	$7.6 \times 10^{-20}$	$6.4 \times 10^{-21}$
	$\text{BR}(H_1^{++} \rightarrow \ell_i^+ \ell_j^+)$	$3.1 \times 10^{-6}$	$1.7 \times 10^{-4}$	0.36	0.12
	$\text{BR}(H_2^{++} \rightarrow W^+W^+)$	$2.7 \times 10^{-20}$	$2.5 \times 10^{-19}$	$3.2 \times 10^{-19}$	$5.7 \times 10^{-20}$
	$\text{BR}(H_2^{++} \rightarrow \ell_i^+ \ell_j^+)$	0.99	0.99	0.99	0.99
	$\sigma(pp \rightarrow H_1^{++}H_1^{--})$	0.93 fb	0.89 fb	0.86 fb	0.75 fb
	$\sigma(pp \rightarrow H_2^{++}H_2^{--})$	2.55 fb	3.35 fb	2.46 fb	2.18 fb
Scenario 3	$\text{BR}(H_1^{++} \rightarrow H_2^{++}h)$	0.99	0.99	not allowed	not allowed
	$\text{BR}(H_1^{++} \rightarrow H_2^+W^+)$	$3.6 \times 10^{-5}$	$1.4 \times 10^{-4}$	0.99	0.99
	$\text{BR}(H_1^{++} \rightarrow W^+W^+)$	$8.6 \times 10^{-14}$	$7.3 \times 10^{-13}$	$1.4 \times 10^{-9}$	$5.8 \times 10^{-10}$
	$\text{BR}(H_1^{++} \rightarrow \ell_i^+ \ell_j^+)$	$4.8 \times 10^{-11}$	$3.7 \times 10^{-11}$	$5.6 \times 10^{-11}$	$4.7 \times 10^{-9}$
	$\text{BR}(H_2^{++} \rightarrow W^+W^+)$	0.02	0.04	0.97	0.05
	$\text{BR}(H_2^{++} \rightarrow \ell_i^+ \ell_j^+)$	0.98	0.96	0.03	0.95
	$\sigma(pp \rightarrow H_1^{++}H_1^{--})$	0.92 fb	0.95 fb	0.84 fb	0.73 fb
	$\sigma(pp \rightarrow H_2^{++}H_2^{--})$	3.42 fb	3.37 fb	2.44 fb	2.15 fb

Table 6: Decay branching ratios and production cross sections for doubly-charged scalars for phase  $\alpha = 45^\circ$ .

$\alpha = 60^\circ$	Mass (GeV)	BP 1	BP 2	BP 3	BP 4
Scenario 1	$H_1^{++}$	557.90	563.51	564.20	556.56
	$H_2^{++}$	412.20	411.51	434.37	439.71
	$H_1^+$	557.62	563.25	559.18	548.00
	$H_2^+$	411.65	411.18	423.27	426.15
Scenario 2	$H_1^{++}$	558.20	565.20	566.40	554.30
	$H_2^{++}$	411.90	413.61	436.56	438.12
	$H_1^+$	558.00	564.50	565.90	553.65
	$H_2^+$	410.75	412.85	435.85	435.32
Scenario 3	$H_1^{++}$	556.65	560.30	567.80	552.90
	$H_2^{++}$	410.25	408.35	437.90	436.59
	$H_1^+$	556.00	559.75	563.21	550.00
	$H_2^+$	409.85	407.80	425.56	429.11

Table 7: Charged scalar masses for phase  $\alpha = 60^\circ$ .

$\alpha = 60^\circ$	Mass (GeV)	BP 1	BP 2	BP 3	BP 4
Scenario 1	$H_{01}$	788.52	796.91	784.64	765.05
	$H_{02}$	788.35	796.27	784.21	764.62
	$H_{03}$	581.43	583.16	579.62	577.78
	$H_{04}$	581.32	582.95	579.13	577.21
	$h$	125.16	125.24	125.14	125.20
Scenario 2	$H_{01}$	790.21	793.82	786.52	762.90
	$H_{02}$	790.00	793.11	786.09	762.42
	$H_{03}$	579.32	580.16	582.32	574.21
	$H_{04}$	579.00	579.92	582.00	573.86
	$h$	125.15	125.10	125.21	125.09
Scenario 3	$H_{01}$	786.51	790.63	785.00	760.71
	$H_{02}$	786.00	790.27	784.32	760.29
	$H_{03}$	577.82	576.21	580.14	570.90
	$H_{04}$	577.50	576.00	579.55	570.58
	$h$	125.23	125.14	125.23	125.18

Table 8: Neutral scalar masses for phase  $\alpha = 60^\circ$ .

$\alpha = 60^\circ$	Data	BP 1	BP 2	BP 3	BP 4
Scenario 1	$\text{BR}(H_1^{++} \rightarrow H_2^{++}h)$	0.99	0.98	0.99	not allowed
	$\text{BR}(H_1^{++} \rightarrow H_2^+W^+)$	$3.9 \times 10^{-4}$	$2.6 \times 10^{-2}$	0.01	0.94
	$\text{BR}(H_1^{++} \rightarrow W^+W^+)$	$1.7 \times 10^{-5}$	$8.9 \times 10^{-3}$	$6.9 \times 10^{-5}$	0.05
	$\text{BR}(H_1^{++} \rightarrow \ell_i^+\ell_j^+)$	$2.6 \times 10^{-22}$	$4.7 \times 10^{-21}$	$3.1 \times 10^{-22}$	$5.6 \times 10^{-20}$
	$\text{BR}(H_2^{++} \rightarrow W^+W^+)$	0.99	0.99	0.99	0.99
	$\text{BR}(H_2^{++} \rightarrow \ell_i^+\ell_j^+)$	$6.7 \times 10^{-19}$	$7.2 \times 10^{-19}$	$5.3 \times 10^{-20}$	$3.5 \times 10^{-15}$
	$\sigma(pp \rightarrow H_1^{++}H_1^{--})$	0.79 fb	0.71 fb	0.72 fb	0.84 fb
	$\sigma(pp \rightarrow H_2^{++}H_2^{--})$	3.22 fb	3.15 fb	2.48 fb	2.51 fb
Scenario 2	$\text{BR}(H_1^{++} \rightarrow H_2^{++}h)$	0.99	0.79	0.99	not allowed
	$\text{BR}(H_1^{++} \rightarrow H_2^+W^+)$	$3.2 \times 10^{-5}$	0.21	$3.1 \times 10^{-3}$	0.88
	$\text{BR}(H_1^{++} \rightarrow W^+W^+)$	$3.9 \times 10^{-22}$	$5.6 \times 10^{-22}$	$5.9 \times 10^{-22}$	$4.3 \times 10^{-22}$
	$\text{BR}(H_1^{++} \rightarrow \ell_i^+\ell_j^+)$	$2.1 \times 10^{-4}$	$1.4 \times 10^{-4}$	$3.7 \times 10^{-4}$	0.12
	$\text{BR}(H_2^{++} \rightarrow W^+W^+)$	$3.2 \times 10^{-19}$	$5.6 \times 10^{-20}$	$7.8 \times 10^{-18}$	$6.3 \times 10^{-19}$
	$\text{BR}(H_2^{++} \rightarrow \ell_i^+\ell_j^+)$	0.99	0.99	0.99	0.99
	$\sigma(pp \rightarrow H_1^{++}H_1^{--})$	0.77 fb	0.74 fb	0.81 fb	0.86 fb
	$\sigma(pp \rightarrow H_2^{++}H_2^{--})$	3.26 fb	3.19 fb	2.46 fb	2.53 fb
Scenario 3	$\text{BR}(H_1^{++} \rightarrow H_2^{++}h)$	0.99	0.90	0.99	not allowed
	$\text{BR}(H_1^{++} \rightarrow H_2^+W^+)$	$2.5 \times 10^{-4}$	0.10	$1.2 \times 10^{-2}$	0.99
	$\text{BR}(H_1^{++} \rightarrow W^+W^+)$	$9.3 \times 10^{-15}$	$2.7 \times 10^{-14}$	$5.3 \times 10^{-11}$	$5.1 \times 10^{-11}$
	$\text{BR}(H_1^{++} \rightarrow \ell_i^+\ell_j^+)$	$6.4 \times 10^{-11}$	$1.7 \times 10^{-12}$	$7.6 \times 10^{-13}$	$2.3 \times 10^{-9}$
	$\text{BR}(H_2^{++} \rightarrow W^+W^+)$	0.03	0.04	0.89	0.02
	$\text{BR}(H_2^{++} \rightarrow \ell_i^+\ell_j^+)$	0.97	0.96	0.11	0.98
	$\sigma(pp \rightarrow H_1^{++}H_1^{--})$	0.81 fb	0.75 fb	0.72 fb	0.83 fb
	$\sigma(pp \rightarrow H_2^{++}H_2^{--})$	3.28 fb	3.20 fb	2.50 fb	2.54 fb

Table 9: Decay branching ratios and production cross sections for doubly-charged scalars for phase  $\alpha = 60^\circ$ .

## 5 Summary and conclusions

We have considered a one-doublet, two-triplet Higgs scenario, with one CP-violating phase in the potential. It is noticed that a larger phase leads to bigger mass-separations between the two doubly-charged mass eigenstates, and also between the states  $H_1^{++}$  and  $H_2^+$ . Consequently, this scenario admits a larger region of the parameter space, when the decay  $H_1^{++} \rightarrow H_2^+ h$  opens up. When it is allowed, this decay often overrides  $H_1^{++} \rightarrow H_2^+ W^+$ . While the role of the latter decay as a characteristic signal of such models was discussed in our earlier work, we emphasize here that the former mode leads to another interesting signal, arising from  $H_1^{++} \rightarrow \ell_i^+ \ell_j^+ h$ . This would mean that the production of SM-like Higgs together with same-sign dileptons peaking at the mass of the lighter doubly-charged scalar. Such a signal, too, may give us a distinctive signature of a two-triplet scenario at the LHC.

**Acknowledgements:** This work has been partially supported by the Department of Atomic Energy, Government of India, through funding available for the Regional Centre for Accelerator-Based Particle Physics, Harish-Chandra Research Institute. We thank Subhadeep Mondal and Nishita Desai for helpful discussions.

## Appendix

The various elements of  $\mathcal{M}_{neut}$ , the neutral scalar mass matrix, are as follows :

$$m_{11} = 2(b_{22} + \frac{1}{2}(e_{22} - h_{22})v^2 + 2(3d_{22}w_2^2 + d_{12}|w_1|^2 \cos 2\alpha + 2(g + g')|w_1|^2)) \quad (41)$$

$$m_{12} = m_{21} = 2b_{12} + (e_{12} - h_{12})v^2 + 4(d_{12} + 2(g + g'))|w_1| \cos \alpha w_2, \quad (42)$$

$$m_{13} = m_{31} = \sqrt{2}v(2t_2 + (e_{12} - h_{12})|w_1| \cos \alpha + (e_{22} - h_{22})w_2), \quad (43)$$

$$m_{14} = m_{41} = 2d_{12}|w_1|^2 \sin 2\alpha, \quad (44)$$

$$m_{15} = m_{51} = -4(d_{12} - 2(g + g'))w_2|w_1| \sin \alpha, \quad (45)$$

$$m_{16} = m_{61} = 0, \quad (46)$$

$$m_{22} = 2(b_{11} + \frac{1}{2}(e_{11} - h_{11})v^2 + (d_{12} + 2(g + g'))w_2^2 + d_{11}|w_1|^2(2\cos^2 \alpha + 1)), \quad (47)$$

$$m_{23} = m_{32} = \sqrt{2}v(2|t_1| \cos \beta + (e_{11} - h_{11})|w_1| \cos \alpha + (e_{12} - h_{12})w_2), \quad (48)$$

$$m_{24} = m_{42} = 4d_{12}w_2|w_1| \sin \alpha, \quad (49)$$

$$m_{25} = m_{52} = 2d_{11}|w_1|^2 \sin 2\alpha, \quad (50)$$

$$m_{26} = m_{62} = 2\sqrt{2}v|t_1| \sin \beta, \quad (51)$$

$$m_{33} = \frac{1}{4}(2a + 6cv^2 + 4|t_1||w_1| \cos(\alpha + \beta) - h_{11}w_1^2 + 4t_2w_2 + 2(e_{12} - h_{12})|w_1| \cos \alpha w_2 + (e_{22} - h_{22})w_2^2 - h_{11}|w_1|^2 \sin^2 \alpha + e_{11}|w_1|^2), \quad (52)$$

$$m_{34} = m_{43} = \sqrt{2}(e_{12} - h_{12})v|w_1| \sin \alpha, \quad (53)$$

$$m_{35} = m_{53} = \sqrt{2}v((e_{11} - h_{11})|w_1| \sin \alpha - 2|t_1| \sin \beta), \quad (54)$$

$$m_{36} = m_{63} = 2|t_1||w_1| \sin(\alpha + \beta), \quad (55)$$

$$m_{44} = 2(b_{22} + \frac{1}{2}(e_{22} - h_{22})v^2 + d_{22}w_2^2 + d_{12}|w_1|^2 \cos 2\alpha + 2(g + g')|w_1|^2), \quad (56)$$

$$m_{45} = m_{54} = 2b_{12} + (e_{12} - h_{12})v^2 + 4d_{12}|w_1| \cos \alpha w_2, \quad (57)$$

$$m_{46} = m_{64} = 4\sqrt{2}t_2v, \quad (58)$$

$$m_{55} = 2(b_{11} + \frac{1}{2}(e_{11} - h_{11})v^2 - 2(d_{12} - 2(g + g'))w_2^2 + 2d_{11}|w_1|^2(2\sin^2 \alpha + 1)), \quad (59)$$

$$m_{56} = m_{65} = 2\sqrt{2}|t_1|v \cos \beta, \quad (60)$$

$$m_{66} = \frac{1}{4}(2a + 2cv^2 - 4|t_1||w_1| \cos(\alpha + \beta) - (e_{11} - h_{11})|w_1|^2 - 4t_2w_2 + 2(e_{12} - h_{12})|w_1|w_2 \cos \alpha + (e_{22} - h_{22})w_2^2), \quad (61)$$

## References

- [1] J. C. Pati and A. Salam, Phys. Rev. D **10** (1974) 275;  
R. N. Mohapatra and J. C. Pati, Phys. Rev. D **11** (1975) 2558;  
G. Senjanović and R. N. Mohapatra, Phys. Rev. D **12** (1975) 1502;  
W. Konetschny, W. Kummer, Phys. Lett. B **70** (1977) 433;  
G. Senjanović, Nucl. Phys. B **153** (1979) 334;  
R. N. Mohapatra, G. Senjanović, Phys. Rev. Lett. **44** (1980) 912;



- J. Schechter and J. W. F. Valle Phys. Rev. D **22**, 2227 (1980);  
T. P. Cheng, L. F. Li, Phys. Rev. D **22**, 2860 (1980);  
M. Magg, C. Wetterich, Phys. Lett. B **94** (1980) 61;  
R. Foot, H. Lew, X. G. He, G. C. Joshi, Z. Phys. C **44** (1989) 441;  
M. Fukugita, T. Yanagida, Physics of Neutrinos and Applications to Astrophysics, Springer, Berlin, Germany, 2003;  
P. Fileviez Perez, JHEP **03** (2009) 142;  
J. Chakrabortty, A. Dighe, S. Goswami, S. Ray, Nucl. Phys. B **820** (2009) 116, arXiv:0812.2776 [hep-ph];  
J. Chakrabortty Phys. Lett. **4B**, 690 (2010);  
G. Senjanović, Int. J. Mod. Phys. A, **26**, 1469 (2011);  
M. Duerr, P. F. Perez and M. Lindner, Phys. Rev. D **88**, 051701 (2013).
- [2] H. Nishiura, K. Matsuda, and T. Fukuyama, Phys. Rev. D **60** (1999) 013006, [hep-ph/9902385];  
E. Kh. Akhmedov, G. C. Branco, and M. N. Rebelo, Phys. Rev. Lett. **84** (2000) 3535, [hep-ph/9912205];  
M. C. Chen and K. T. Mahanthappa, Phys. Rev. D **62** (2000) 113007, [hep-ph/0005292];  
S. K. Kang and C. S. Kim, Phys. Rev. D **63** (2001) 113010, [hep-ph/0012046];  
P.H. Frampton, S.L. Glashow, D. Marfatia, Phys. Lett. B **536**, 79 (2002) [hep-ph/0201008];  
Z.-Z. Xing, Phys. Lett. B **530** (2002) 159 [hep-ph/0201151];  
Z.-Z. Xing, Phys. Lett. B **539**, 85 (2002) [hep-ph/0205032];  
M. Honda, S. Kaneko and M. Tanimoto, JHEP **0309**, 028 (2003) [hep-ph/0303227];  
B. R. Desai, D. P. Roy, and A. R. Vaucher, Mod. Phys. Lett. A. **18** (2003) 1355, [hep-ph/0209035].  
W.-L. Guo and Z.-Z. Xing, Phys. Lett. B **583**, 163 (2004) [hep-ph/0310326];  
M. Honda, S. Kaneko and M. Tanimoto, Phys. Lett. B **593**, 165 (2004) [hep-ph/0401059].  
W. Grimus and L. Lavoura, J. Phys. G **31**, 693 (2005) [hep-ph/0412283].
- [3] A. Chaudhuri, W. Grimus and B. Mukhopadhyaya, JHEP **02**, 060 (2014) [arXiv:1305.5761 [hep-ph]].
- [4] W. Grimus, R. Pfeiffer and T. Schwetz, Eur. Phys. J. C **13**, 125 (2000) [hep-ph/9905320].
- [5] N. G. Deshpande and E. Ma, Phys. Rev. D **18** 2574 (1078).
- [6] S. Choubey, W. Rodejohann and P. Roy, Nucl.Phys. B **808** (2009), arXiv:0807.4289 [hep-ph];  
B. Adhikary, A. Ghosal and P. Roy JHEP 0910 (2009) **040**, arXiv:0908.2686 [hep-ph];  
P. O. Ludl and W. Grimus, JHEP 1407 (2014) **090**, arXiv:1406.3546 [hep-ph];  
J. Liao, D. Marfatia and K. Whisnant, Nucl.Phys. B **900** (2015), arXiv:1508.07364 [hep-ph];  
H. Fritzsch, Mod.Phys.Lett. A **30** (2015) 28, 1550138,  
L. M. Cebola, D. E. -Costa and R. G. Felipe, Phys.Rev. D **92** (2015) 2, 025005,

- arXiv:1504.06594 [hep-ph];  
L. Lavoura , J.Phys. G **42** (2015) 105004, arXiv:1502.03008 [hep-ph];  
A. Ghosal and R. Samanta, JHEP 1505 (2015) **077** , arXiv:1501.00916 [hep-ph];  
P. O. Ludl and W. Grimus, Phys. Lett. B **744** (2015), arXiv:1501.04942 [hep-ph] .
- [7] P. Minkowski, Phys. Lett. B **67** (1977) 421;  
T. Yanagida, in Proceedings of the workshop on unified theories and baryon number in the universe (Tsukuba, Japan, 1979), edited by O. Sawada, A. Sugamoto (Tsukuba: KEK report 79-18, 1979);  
S. L. Glashow, in Quarks and leptons, Proceedings of the advanced study institute (Carg'ese, Corsica, 1979), edited by J. L. Basdevant *et al.* (Plenum, New York 1981);  
M. Gell-Mann, P. Ramond, R. Slansky, in Supergravity, edited by D. Z. Freedman, F. van Nieuwenhuizen (North Holland, Amsterdam 1979);  
R. N. Mohapatra, G. Senjanović, Phys. Rev. Lett. **44** (1980) 912;  
P. H. Frampton, S. L. Glashow, D. Marfatia, Phys. Lett. B **536** (2002) 79, [hep-ph/0201008];  
W. Grimus, A. S. Joshipura, L. Lavoura and M. Tanimoto, Eur. Phys. J. C **36**, 227 (2004) [hep-ph/0405016]  
M. Maltoni, T. Schwetz, M. Tortola, J. W. F. Valle, New J. Phys. **6** (2004) 122, [hep-ph/0405172].  
W. Grimus, in Lectures on Flavor Physics, edited by U.-G. Meiner, W. Plessas (Springer-Verlag, New York 2004), p. **169**, [hep-ph/0307149];  
W. Grimus and L. Lavoura, J. Phys. G **31**, 693 (2005) [hep-ph/0412283];
- [8] J. Beringer *et al.* (Particle Data Group), Phys. Rev. D **86**, 010001 (2012).
- [9] G. L. Fogli, E. Lisi, A. Marrone, D. Montanino, A. Palazzo and A. M. Rotunno, Phys. Rev. D **86**, 013012 (2012) [arXiv:1205.5254 [hep-ph]].
- [10] Daya Bay Collaboration, F. P. An *et al.* Phys. Rev. Lett. **108**, 171803 (2012) [arXiv:1203.1669 [hep-ex]].
- [11] RENO Collaboration, J. K. Ahn *et al.*, Phys. Rev. Lett. **108**, 191802 (2012) [arXiv:1204.0626 [hep-ex]].
- [12] N. D. Christensen and C. Duhr, Comput. Phys. Commun. **180**, 1614 (2009) [arXiv:0806.4194 [hep-ph]].
- [13] C. Degrande, C. Duhr, B. Fuks, D. Grellscheid, O. Mattelaer and T. Reiter, Comput. Phys. Commun. **183**, 1201 (2012) [arXiv:1108.2040 [hep-ph]].
- [14] J. Alwall, R. Frederix, S. Frixione, V. Hirschi, F. Maltoni, O. Mattelaer, H. S. Shao, T. Stelzer, P. Torrielli and M. Zaro, JHEP 1407 (2014) **079**, arXiv:1405.0301 [hep-ph].